

# Heavy Petroleum Composition. 1. Exhaustive Compositional Analysis of Athabasca Bitumen HVGO Distillates by Fourier Transform Ion Cyclotron Resonance Mass Spectrometry: A Definitive Test of the Boduszynski Model

Amy M. McKenna,<sup>†,‡</sup> Jeremiah M. Purcell,<sup>†,§</sup> Ryan P. Rodgers,<sup>\*,†,‡</sup> and Alan G. Marshall<sup>\*,†,‡</sup>

<sup>†</sup>National High Magnetic Field Laboratory, Florida State University, 1800 East Paul Dirac Drive, Tallahassee, Florida 32310-4005, and <sup>‡</sup>Department of Chemistry and Biochemistry, Florida State University, 95 Chieftain Way, Tallahassee, Florida 32306 <sup>§</sup>Current Address: Shell Global Solutions, Westhollow Technology Center, Houston, TX 77082.

Received February 5, 2010. Revised Manuscript Received April 18, 2010

Fourier transform ion cyclotron resonance mass spectrometry (FT-ICR MS) allows detailed characterization of complex petroleum samples at the level of elemental composition assignment. Ultrahigh-resolution (450 000–650 000 at  $m/z$  500) enables identification of isobaric species that differ in mass by 3 mDa or less, and high mass accuracy (mass error of better than 300 ppb), combined with Kendrick mass sorting, allows for unambiguous molecular formula assignment to each of more than 10 000–20 000 peaks in each mass spectrum. Thus, it is possible to identify, sort, and monitor thousands of elemental compositions simultaneously, as a function of the boiling point. Here, the detailed FT-ICR MS characterization of an Athabasca bitumen heavy vacuum gas oil (HVGO) distillation series exposes the progression of heteroatom class, type (double bond equivalents (DBE), number of rings plus double bonds to carbon), and carbon number for tens of thousands of crude oil species, as a function of the boiling point. Specifically, we analyze a distillation series of Athabasca bitumen HVGO with cut temperatures from the initial boiling point (IBP) to 538 °C (in eight cuts) by atmospheric pressure photoionization (APPI), as well as positive and negative electrospray ionization (ESI) FT-ICR MS, to determine the distributions of nonpolar and polar species, as a function of the HVGO boiling point. Compositional distributions reveal definitive heteroatom class, type, and carbon number trends among distillation cuts, and provide the first detailed compositional evidence in support of the Boduszynski model that describes the progression of petroleum composition and structure as a function of the boiling point. Quantitation of the aromaticity and carbon number profiles of both polar and nonpolar species in all distillate cuts further affirms the validity of the Boduszynski model for the HVGO distillate range, and provides evidence for cycloalkane linkages, in addition to polyaromatic cores.

## Introduction

The acceptance of heavy refinery feeds requires the extension and improvement of analytical techniques routinely used for light feeds to the characterization of heavy feeds.<sup>1</sup> However, the task is daunting, given the increased compositional complexity encountered in heavy crude oils and higher boiling distillate cuts. The increased complexity arises from the progression of narrow molecular weight ranges (in light distillate cuts) to broader molecular weight distributions with higher heteroatom contents for heavy crudes and distillates. Generally, molecules progress from single heteroatom-containing compounds in the middle distillate fractions to multiheteroatom-containing compounds in the vacuum residue. Distillation is an important refinery process to reduce crude oil compositional complexity and produce meaningful product yields for species in each boiling range,

and to predict problems encountered during processing.<sup>2–5</sup> Longstanding analytical techniques for characterizing compositional diversity in individual boiling cuts include gel permeation chromatography (GPC)<sup>6</sup> and high-performance liquid chromatography (HPLC)<sup>7</sup> to discern compositional changes in distillate fractions in refinery processes. Recently, two-dimensional gas chromatography (GC × GC) has characterized and quantitated lighter distillate fractions in crude oil.<sup>8–10</sup> Thermogravimetry<sup>11</sup> and nuclear magnetic resonance<sup>12–14</sup> have been applied to

\* Authors to whom correspondence should be addressed. Tel.: +1 850 644 0529 (AGM), +1 850 644 2398 (RPR). Fax: +1 850 644 1366. E-mail addresses: marshall@magnet.fsu.edu (AGM), rogers@magnet.fsu.edu (RPR).

(1) Speight, J. G. *Handbook of Petroleum Analysis*; Chemical Analysis: A Series of Monographs on Analytical Chemistry and its Applications; Winefordner, J. D., Ed.; Wiley Interscience: New York, 2001; Vol. 158.

(2) Boduszynski, M. M. *Energy Fuels* **1987**, *1* (1), 2–11.

(3) Boduszynski, M. M. *Energy Fuels* **1988**, *2* (5), 597–613.

(4) Boduszynski, M. M.; Altgelt, K. H. *Energy Fuels* **1992**, *6* (1), 72–76.

(5) Boduszynski, M. M.; Altgelt, K. H. *Energy Fuels* **1992**, *6* (1), 68–72.

(6) Coleman, H. J.; Hirsch, D. E.; Dooley, J. E. *Anal. Chem.* **1969**, *41* (6), 800–804.

(7) Sullivan, R. F.; Boduszynski, M. M.; Fetzer, J. C. *Energy Fuels* **1989**, *3*, 603–612.

(8) Frysinger, G. S.; Gaines, R. B.; Reddy, C. M. *Environ. Forensics* **2002**, *3*, 27–34.

(9) Mullins, O. C.; Ventura, G. T.; Nelson, R. K.; Betancourt, S. S.; Raghuraman, B.; Reddy, C. M. *Energy Fuels* **2008**, *22*, 496–503.

(10) Reddy, C. M.; Nelson, R. K.; Sylva, S. P.; Xu, L.; Peacock, E. A.; Raghuraman, B.; Mullins, O. C. *J. Chromatogr., A* **2007**, *1148*, 100–107.

(11) Goncalves, M. L. A.; Ribeiro, D. A.; da Mota, D. A. P.; Teixeira, A. M. R. F.; Teixeira, M. A. G. *Fuel* **2006**, *85*, 1151–1155.

(12) Clutter, D. R.; Petrakis, L.; Stenger, R. L., Jr.; Jensen, R. K. *Anal. Chem.* **1972**, *44* (8), 1395–1405.

(13) Vishnoi, V.; Agrawal, K. M.; Singh, I. D.; Raizada, B. B. *Pet. Sci. Technol.* **2005**, *23*, 931–937.

(14) Zhao, S.; Kotlyar, L. S.; Woods, J. R.; Sparks, B. D.; Chung, K. H. *Pet. Sci. Technol.* **2000**, *18* (5&6), 587–606.

evaluate medium and heavy fractions of crude oil. However, high-boiling fractions and vacuum residues are often separated by supercritical fluid extraction and fractionation coupled with Fourier transform infrared (FTIR), nuclear magnetic resonance (NMR), and X-ray photoelectron spectroscopy (XPS) for compositional characterization.<sup>15–17</sup> Nevertheless, most analytical techniques access only lower boiling fractions, because of the increase in compositional complexity that accompanies an increase in the boiling point, and/or measure only bulk properties in heavy crudes or heavy distillate fractions.

Mass spectrometry (MS) provides detailed characterization of crude oil composition and has been coupled to ionization/separation<sup>18–21</sup> techniques such as gas chromatography-MS,<sup>22–24</sup> supercritical fluid chromatography,<sup>25,26</sup> field ionization,<sup>2–4,27,28</sup> field desorption,<sup>29–31</sup> electron ionization,<sup>32,33</sup> and electrospray ionization.<sup>29,30</sup> Zhan and Fenn first applied electrospray ionization mass spectrometry (ESI-MS) to the analysis of polar molecules in petroleum distillates, but they lacked sufficient resolving power for complete compositional assignment (a problem common to all but the highest-resolution mass spectrometers).<sup>34</sup> Since then, electrospray ionization coupled to ultrahigh-resolution Fourier transform ion cyclotron resolution mass spectrometry (FT-ICR MS)

has extensively characterized the polar species in petroleum.<sup>30,35–41</sup> Although polar compounds represent a small fraction (0%–15%) of the total species present in petroleum, they are implicated in production issues such as corrosion, and catalyst deactivation/fouling in upgrading processes such as hydrotreatment.<sup>42</sup> Thus, electrospray ionization *selectively* ionizes acidic and basic polar heterocompounds from the hydrocarbon matrix of petroleum samples with little or no matrix effects<sup>43</sup> and, as a result, is widely accepted as the preferred ionization technique for *polar* compound characterization by mass spectrometry.

For *nonpolar* species, field ionization/desorption has historically been used to characterize heavy vacuum gas oil (HVGO) and other heavy distillate fractions.<sup>30</sup> However, field desorption is a pulsed ionization source and ionization occurs in vacuo, necessitating tedious replacement of emitters and time-consuming data collection. Atmospheric pressure photoionization (APPI) was first used as an ionization method for mass spectrometry by Robb et al.,<sup>44</sup> with toluene as a dopant to increase analyte ionization efficiency.<sup>45</sup> Subsequently, APPI has analyzed a wide range of compounds, including pharmaceutical and medicinal drugs,<sup>46–49</sup> lipids,<sup>50,51</sup> polyaromatic hydrocarbons,<sup>52–54</sup> explosives,<sup>55</sup> and steroids.<sup>56–58</sup> APPI was first coupled to FT-ICR MS for analysis of corticosteroids.<sup>59</sup> Purcell et al. first coupled APPI to FT-ICR MS for characterization of nonpolar species in crude oil and resolved and identified more than 12 000 unique elemental compositions across a 400 Da mass window.<sup>60–63</sup> APPI FT-ICR MS has recently been used to identify and characterize vanadyl

(15) Zhao, S.; Xu, Z.; Xu, C.; Chung, K. H. *J. Pet. Sci. Eng.* **2004**, *41*, 233–242.

(16) Zhao, S.; Sparks, B. D.; Kotlyar, L. S.; Chung, K. H. *Catal. Today* **2007**, *125*, 122–136.

(17) Zhao, S.; Xu, Z.; Xu, C.; Chung, K. H.; Wang, R. *Fuel* **2004**, *84*, 635–645.

(18) Robbins, W. K. *J. Chromatogr. Sci.* **1998**, *36* (9), 457–466.

(19) Barman, B. N. *Energy Fuels* **2005**, *19*, 1995–2000.

(20) Coleman, H. J.; Hirsch, D. E.; Dooley, J. E. *Anal. Chem.* **1969**, *41* (6), 800–804.

(21) Takeuchi, T.; Ishii, D. *J. High Resolut. Chromatogr.* **1983**, *6*, 310–315.

(22) Roehner, R. M.; Fletcher, J. V.; Hanson, F. V.; Dahdah, N. F. *Energy Fuels* **2002**, *16* (1), 211–217.

(23) Wang, Z.; Fingas, M.; Li, K. *J. Chromatogr. Sci.* **1990**, *32*, 361–382.

(24) Morgan, T. J.; George, A.; Avarez, P.; Herod, A. A.; Kandiyoti, R.; Morgan, T. J. *Energy Fuels* **2008**, *22* (5), 3275–3292.

(25) Qian, K.; Diehl, J. W.; Dechert, G. J.; DiSanzo, F. P. *Eur. J. Mass Spectrom.* **2004**, *10* (2), 187–196.

(26) Wright, B. W.; Smith, R. D. *Org. Geochem.* **1989**, *14* (2), 227–232.

(27) Altgelt, K. H.; Boduszynski, M. M. *Energy Fuels* **1992**, *6* (1), 68–72.

(28) Boduszynski, M. M. *Liq. Fuels Technol.* **1984**, *2* (3), 211–232.

(29) Stanford, L. A.; Kim, S.; Rodgers, R. P.; Marshall, A. G. *Energy Fuels* **2006**, *20*, 1664–1673.

(30) Smith, D. F.; Rahimi, P.; Teclemariam, A.; Rodgers, R. P.; Marshall, A. G. *Energy Fuels* **2008**, *22* (5), 3118–3125.

(31) Qian, K.; Edwards, K. E.; Siskin, M.; Olmstead, W. N.; Mennito, A. S.; Dechert, G. J.; Hoosain, N. E. *Energy Fuels* **2007**, *21*, 1042–1047.

(32) Guan, S.; Marshall, A. G.; Scheppele, S. E. *Anal. Chem.* **1996**, *68*, 46–71.

(33) Fu, J. M.; Klein, G. C.; Smith, D. F.; Kim, S.; Rodgers, R. P.; Hendrickson, C. L.; Marshall, A. G. *Energy Fuels* **2006**, *20* (3), 1235–1241.

(34) Zhan, D. L.; Fenn, J. B. *Int. J. Mass Spectrom.* **2000**, *194* (2–3), 197–208.

(35) Qian, K.; Robbins, W. K.; Hughey, C. A.; Cooper, H. J.; Rodgers, R. P.; Marshall, A. G. *Energy Fuels* **2001**, *15* (6), 1505–1511.

(36) Wu, Z.; Jernström, S.; Hughey, C. A.; Rodgers, R. P.; Marshall, A. G. *Energy Fuels* **2003**, *17* (4), 946–953.

(37) Hughey, C. A.; Rodgers, R. P.; Marshall, A. G. *Anal. Chem.* **2002**, *74* (16), 4145–4149.

(38) Stanford, L. A.; Rodgers, R. P.; Marshall, A. G.; Czarnecki, J.; Wu, X. A. *Energy Fuels* **2007**, *21* (2), 973–981.

(39) Kim, S.; Stanford, L. A.; Rodgers, R. P.; Marshall, A. G.; Walters, C. C.; Qian, K.; Wenger, L. M.; Mankiewicz, P. *Org. Geochem.* **2005**, *36*, 1117–1134.

(40) Smith, D. F.; Schaub, T. M.; Rahimi, P.; Teclemariam, A.; Rodgers, R. P.; Marshall, A. G. *Energy Fuels* **2007**, *21* (3), 1309–1316.

(41) Wu, Z.; Rodgers, R. P.; Marshall, A. G.; Strohm, J. J.; Song, C. *Energy Fuels* **2005**, *19* (3), 1072–1077.

(42) Schaub, T. M.; Jennings, D. W.; Kim, S.; Rodgers, R. P.; Marshall, A. G. *Energy Fuels* **2007**, *21* (1), 185–194.

(43) Hughey, C. A.; Rodgers, R. P.; Marshall, A. G.; Qian, K.; Robbins, W. K. *Org. Geochem.* **2002**, *33* (7), 743–759.

(44) Robb, D. B.; Covey, T. R.; Bruins, A. P. *Anal. Chem.* **2000**, *72* (15), 3653–3659.

(45) Robb, D. B.; Blades, M. W. *J. Am. Soc. Mass Spectrom.* **2006**, *17*, 130–139.

(46) Cai, Y.; Kingery, D.; McConnell, O.; Bach, A. C., II. *Rapid Commun. Mass Spectrom.* **2005**, *19* (12), 1717–1724.

(47) Wang, G.; Hsieh, Y.; Korfmacher, W. A. *Anal. Chem.* **2005**, *77* (2), 541–548.

(48) Cai, S.-S.; Hanold, K. A.; Syage, J. A. *Anal. Chem.* **2007**, *79* (6), 2491–2498.

(49) Silva, L. C.; Oliveira, L. S. O. B.; Mendes, G. D.; Garcia, G.; dos Santos Pereira, A.; De Nucci, G. *J. Chromatogr. B* **2006**, *832* (2), 302–306.

(50) Müller, A.; Mickel, M.; Geyer, R.; Ringseis, R.; Eder, K.; Steinhart, H. *J. Chromatogr. B* **2006**, *837* (1–2), 147–152.

(51) Cai, S.-S.; Syage, J. A. *Anal. Chem.* **2006**, *78* (4), 1191–1199.

(52) Cai, S.-S.; Syage, J. A.; Hanold, K. A.; Balogh, M. P. *Anal. Chem.* **2009**, *81* (6), 2123–2128.

(53) Itoh, N.; Narukawa, T.; Numata, M.; Aoyagi, Y.; Yarita, T.; Takatsu, A. *Polycyclic Aromat. Compd.* **2009**, *29* (1), 41–55.

(54) Smith, D. F.; Robb, D. B.; Blades, M. W. *J. Am. Soc. Mass Spectrom.* **2009**, *20* (1), 73–79.

(55) Song, L.; Bartmess, J. E. *Rapid Commun. Mass Spectrom.* **2009**, *23* (1), 77–84.

(56) Leinonen, A.; Kuuranne, T.; Kostianen, R. *J. Mass Spectrom.* **2002**, *37* (7), 693–698.

(57) Roy, S.; Delobel, A.; Gaudin, K.; Touboul, D.; Germain, D. P.; Baillet, A.; Prognon, P.; Laprévotte, O.; Chaminade, P. *J. Chromatogr. A* **2006**, *1117* (2), 154–162.

(58) Karuna, R.; von Eckardstein, A.; Rentsch, K. M. *J. Chromatogr. A* **2009**, *877* (3), 261–268.

(59) Greig, M. J.; Bolanos, B.; Quenzer, T.; Bylund, J. M. R. *Rapid Commun. Mass Spectrom.* **2003**, *17*, 2763–2768.

(60) Purcell, J. M.; Hendrickson, C. L.; Rodgers, R. P.; Marshall, A. G. *Anal. Chem.* **2006**, *78* (16), 5906–5912.

(61) Purcell, J. M.; Hendrickson, C. L.; Rodgers, R. P.; Marshall, A. G. *J. Am. Soc. Mass Spectrom.* **2007**, *18* (9), 1682–1689.

(62) Purcell, J. M.; Juyal, P.; Kim, D. G.; Rodgers, R. P.; Hendrickson, C. L.; Marshall, A. G. *Energy Fuels* **2007**, *21* (5), 2869–2874.

(63) Purcell, J. M.; Rodgers, R. P.; Hendrickson, C. L.; Marshall, A. G. *J. Am. Soc. Mass Spectrom.* **2007**, *18* (7), 1265–1273.

porphyrins in unfractionated asphaltene and whole crude oil, and the nebulization temperature has been correlated to the boiling point range in heavy crude oil.<sup>64,65</sup> Although it does not efficiently ionize purely alkane species, APPI is ideally suited for coupling to high-resolution FT-ICR MS, because APPI is a continuous atmospheric pressure ion source with little or no down time between sample analyses.

Boduszynski et al. conducted a prescient, noteworthy comprehensive analysis of heavy crude oil composition in the late 1980s and early 1990s.<sup>2–5</sup> Their series of papers was unique because, unlike crude oil models/reaction networks that were based on compositional analysis of a *target* crude,<sup>66–68</sup> Boduszynski and Altgelt proposed a model based on the progression of crude oil composition and molecular weight as a function of boiling point, and proposed an extrapolation to an upper limit of molecular weight for *all* crudes. Remarkably, if expanded to encompass current collective compositional predictions, the Boduszynski/Altgelt model (which is now 20 years old) predicts what is now known as the Petroleome. Combined with Quann and Jaffe, early contributions in the development of composition-dependent models for specific crudes have pioneered the current field of “Petroleomics”.<sup>69–72</sup>

The objective of the current work is fundamental. Oil companies sell molecules; therefore, an oil’s composition determines its economic value. The ultimate goal of the detailed speciation of all the components of crude oil is simply a model to predict (for example) phase, deposition, distillation, and upgrading behavior, as well as bulk properties such as viscosity. However, even methods and results used to obtain *bulk* properties for heavy ends and asphaltenes are hotly debated. Therefore, rather than attempting to generate a predictive model directly from the exhaustive detailed composition of a *specific* heavy crude, we instead begin from a 20 year-old petroleum composition model that presumes to describe *all* crudes, and evaluate whether or not the exhaustive compositional analysis of whole fractions and narrow distillation cuts (which span the heavy vacuum gas oil (HVGO) range centered in Boduszynski’s model (see Figure 1)) supports the Boduszynski model. This simple but important issue can

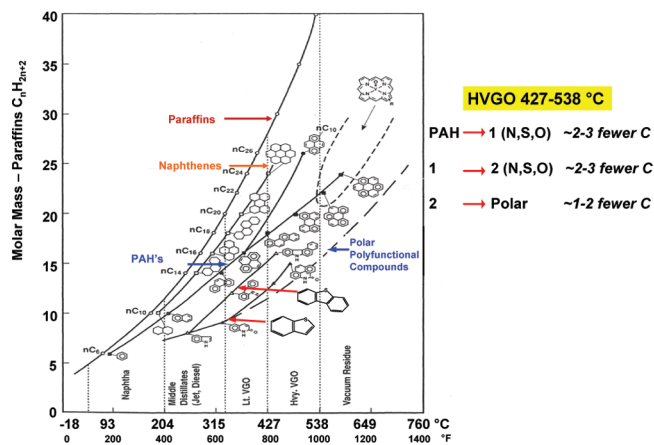


**Figure 1.** Boduszynski and Altgelt model illustrating representation of the effect of molecular weight (left) and structure (right) on atmospheric equivalent boiling point (AEBP), for compounds known to exist in crude oil.<sup>84</sup> At a given boiling point, the carbon number decreases as heteroatom content increases for compounds in the HVGO boiling range: pure hydrocarbons have ~2–3 more carbon atoms than mono-heteroatomic analogues; addition of a second heteroatom reduces the carbon number by another 2–3. Polar functional groups exhibit the lowest carbon number within each boiling range.

appropriately focus future research efforts and put an end to controversy about the molecular weight of petroleum.<sup>24,73–83</sup>

Boduszynski related the atmospheric equivalent boiling point to the molecular weight/structure for heavy crude oil distillate fractions and concluded that (all) crude oil compositions are continuous in molecular weight, structure, and heteroatoms (N, O, and S) in the distillables and made the inductive leap that the same trend extends to asphaltenes and nondistillable residues.<sup>2–4,28,84</sup> Based on his model, which was developed from boiling point trends of standards and backed by mass spectrometric results for a collection of heavy crude oils, Boduszynski concluded that “*most of petroleum components do not exceed a molecular weight of about 2000*”. He acknowledged that the results are controversial:

“These findings are significant because of the existing controversy over whether there is an appreciable concentration of molecules in petroleum having molecular weights greater than 2000 Da. Data show there is not.” Subsequently, an increasing number of bulk measurements support his original claim.<sup>80,85–93</sup> Nevertheless, 20 years later,

(64) McKenna, A. M.; Purcell, J. M.; Rodgers, R. P.; Marshall, A. G. *Energy Fuels* **2009**, *23*, 2122–2128.

(65) McKenna, A. M.; Purcell, J. M.; Rodgers, R. P.; Rahimi, P.; Marshall, A. G. Correlation of distillation and nebulization temperature of bitumen by use of atmospheric pressure photoionization Fourier transform ion cyclotron resonance mass spectrometry. In *Abstracts of Papers, 235th ACS National Meeting*, New Orleans, LA, April 6–10, 2008; American Chemical Society: Washington, DC, 2008.

(66) Quann, R. J.; Jaffe, S. B. *Ind. Eng. Chem. Res.* **1992**, *31* (11), 2483–2497.

(67) Quann, R. J.; Jaffe, S. B. *Chem. Eng. Sci.* **1996**, *51* (10), 1615–1635.

(68) Jaffe, S. B.; Freund, H.; Olmstead, W. N. *Ind. Eng. Chem. Res.* **2005**, *44* (26), 9840–9852.

(69) Marshall, A. G.; Rodgers, R. P. *Acc. Chem. Res.* **2004**, *37* (1), 53–59.

(70) Rodgers, R. P.; Marshall, A. G. Petroleomics: Advanced Characterization of Petroleum-Derived Materials Characterized by Fourier Transform Ion Cyclotron Resonance Mass Spectrometry (FT-ICR MS). In *Asphaltenes, Heavy Oils and Petroleomics*; Mullins, O. C., Sheu, E. Y., Hammami, A., Marshall, A. G., Eds.; Springer: New York, 2006; pp 63–93.

(71) Rodgers, R. P.; Marshall, A. G. *Proc. Natl. Acad. Sci. U.S.A.* **2008**, *105* (47), 1–6.

(72) Rodgers, R. P.; Schaub, T. M.; Marshall, A. G. *Anal. Chem.* **2005**, *77* (1), 20A–27A.

(73) Herod, A. A.; Bartle, K. D.; Kandiyoti, R. *Energy Fuels* **2008**, *22* (6), 4312–4317.

(74) Herod, A. A.; Kandiyoti, R. *Energy Fuels* **2008**, *22* (6), 4307–4309.

(75) Mullins, O. C. *Fuel* **2006**, *86* (1–2), 309–312.

(76) Guerra, R.; Ladavac, K.; Andrews, A.; Mullins, O.; Sen, P. *Fuel* **2007**, *86* (12–13), 2016–2020.

(77) Mullins, O. C.; Matinez-Haya, B.; Marshall, A. G. *Energy Fuels* **2008**, *22* (3), 1765–1773.

(78) Behrouzi, M.; Luckman, P. F. *Energy Fuels* **2008**, *22* (3), 1792–1798.

(79) Herod, A. A.; Kandiyoti, R.; Bartle, K. D. *Fuel* **2006**, *85*, 1950–1951.

(80) Badre, S.; Gonçalves, C. C.; Norinaga, K.; Gustavson, G.; Mullins, O. C. *Fuel* **2006**, *85*, 1–11.

(81) Morgan, T. J.; Millan, M.; Behrouzi, M.; Herod, A. A.; Kandiyoti, R. *Energy Fuels* **2005**, *19* (1), 164–169.

(82) Strausz, O. P.; Safarik, I.; Lown, E. M.; Morales-Izquierdo, A. *Energy Fuels* **2008**, *22* (2), 1156–1166.

(83) Mullins, O. C. *Energy Fuels* **2009**, *23*, 2845–2854.

(84) Boduszynski, M. M.; Altgelt, K. H. *Composition and Analysis of Heavy Petroleum Fractions*; CRC Press: New York, 1994.

(85) Betancourt, S. S.; Ventura, G. T.; Pomerantz, A. E.; Vilorio, O.; Dubost, F. X.; Zuo, J.; Monson, G.; Bustamante, D.; Purcell, J. M.; Nelson, R. K.; Rodgers, R. P.; Reddy, C. M.; Marshall, A. G.; Mullins, O. C. *Energy Fuels* **2009**, *23* (3), 1178–1188.

(86) Betancourt, S. S.; Ventura, G. T.; Pomerantz, A. E.; Vilorio, O.; Dubost, F. X.; Zuo, J.; Monson, G.; Bustamante, D.; Purcell, J. M.; Nelson, R. K.; Rodgers, R. P.; Reddy, C. M.; Marshall, A. G.; Mullins, O. C. *Fuel* **2003**, *82* (9), 1075–1084.

(87) Buenrostro-Gonzalez, E.; Groenzin, H.; Lira-Galeana, C.; Mullins, O. C. *Energy Fuels* **2001**, *15* (4), 972–978.



petroleum science remains bogged down in the same arguments about petroleum molecular weight. A definitive proof of Boduszynski's model requires direct, complete compositional characterization of complex distillate cuts unavailable at that time. If substantiated, the Boduszynski model could impose strict limits on molecular weight distributions for both distillable and nondistillable petroleum fractions that contradict many previously published assertions about petroleum molecular weight and composition.<sup>94–98</sup> Although distillation separates components based on volatility and thereby limits the observable carbon number and aromaticity, each distillate fraction nevertheless remains compositionally complex and contains a wide variety of different heteroatom functionalities.<sup>4</sup> Therefore, detailed compositional characterization of each fraction is paramount to understand the structural progression of crude oil compounds as a function of boiling point: from the economically beneficial, low-boiling fractions (e. g., gasoline) to the problematic, high-boiling and nondistillable fractions (e.g., resids and asphaltenes). Such detailed characterization is now possible with a single analytical technique: FT-ICR MS.

The inherent high resolution and mass accuracy of FT-ICR MS make it an effective tool for compositional analysis of complex mixtures such as heavy crude oil and distillate fractions. Here, we analyze an Athabasca bitumen HVGO distillation series (fractions critical to Boduszynski's model) to characterize nonpolar and polar species enabling characterization of molecular composition as a function of boiling point. We compare detailed compositional results obtained for polar species by electrospray ionization (ESI) and nonpolar species by APPI coupled to FT-ICR mass spectrometry to access the validity of the model proposed by Boduszynski et al. in the HVGO boiling range.<sup>2–4,27</sup> The current results are the first of a five-part series of publications on the composition of heavy petroleum and asphaltenes.

### Experimental Methods

**Sample Preparation.** A bitumen heavy vacuum gas oil (HVGO) was fractionated by following the ASTM D-1160 standard into eight distillate fractions: (IBP–343 °C, 343–375 °C, 375–400 °C, 400–425 °C, 425–450 °C, 450–475 °C, 475–500 °C, and 500–538 °C). Additional distillation information can be found elsewhere.<sup>30</sup> Each distillate fraction (~10 mg) was diluted with 5 mL of toluene (HPLC grade, Sigma–Aldrich Chemical Co., St. Louis, MO) to make a stock solution (2 mg/mL) that was either further diluted to yield a final concentration of 500 µg/mL for APPI or diluted with equal parts (vol:vol)

methanol spiked with 2% (by volume) ammonium hydroxide (negative ESI) or formic acid (positive ESI) FT-ICR MS analysis.

**Instrumentation.** *APPI Source.* Samples were ionized with an Ion Maxx API source (ThermoFisher Corp., Bremen, Germany) in photoionization configuration. The sample flows through a fused-silica capillary at a rate of 50 µL/min and is mixed with nebulization gas (N<sub>2</sub>, introduced at a pressure of ~100 kPa) inside a heated vaporizer operated between 250 and 350 °C. Nitrogen served as an auxiliary and sheath gas and was regulated by Xcaliber software (set to 50 and 5 arbitrary units, respectively). Source parameters were set in Xcaliber as follows: sweep gas rate, 5 arbitrary units; capillary voltage, 11 V; tube lens, 50 V. Once nebulized, the sample exits the vaporizer in a confined jet and flows orthogonal to the krypton VUV lamp that produces 10 eV photons (120 nm), where photoionization occurs at atmospheric pressure. Ions are then swept into the first pumping stage of the mass spectrometer by differential pressure through a heated metal capillary. Toluene is used as a solvent/dopant to increase analyte ionization through proton-transfer and charge exchange reactions.<sup>44</sup> Electrospray ions were generated externally by a microelectrospray source<sup>99</sup> and were delivered by a syringe pump at a rate of 500 nL/min. A potential of 2.5 kV was applied between the capillary needle and the ion entrance to the mass spectrometer.

**14.5 T FT-ICR MS.** Low resolution and high resolution mass spectra were collected with a customized hybrid linear quadrupole ion trap/FT-ICR MS (LTQ-FT, ThermoFisher Corp., Bremen, Germany) adapted to operate in an actively shielded 14.5 T superconducting magnet (Magnex, Oxford, UK), as described in detail elsewhere.<sup>100</sup> The octopole directly behind the LTQ was modified to include tilted wire extraction electrodes and serves as a secondary ion accumulation method and improves ion injection efficiency.<sup>101</sup> Ions may be mass selected in the LTQ and accumulated in the wired octopole for numerous cycles before the entire octopole ion population is transferred to the ICR cell for excitation and detection.

**Mass Calibration and Data Analysis.** Positive-ion APPI FT-ICR mass spectra were internally calibrated,<sup>102,103</sup> with respect to a highly abundant homologous alkylation series containing one <sup>32</sup>S atom, and verified by identification of the corresponding <sup>34</sup>S signal at the correct relative abundance. Singly charged ions with a relative abundance greater than six standard deviations of baseline rms noise (6σ) were exported to a spreadsheet, after conversion to the Kendrick mass scale<sup>104</sup> for easier identification of homologous series. For each elemental composition, C<sub>c</sub>H<sub>h</sub>N<sub>n</sub>O<sub>o</sub>S<sub>s</sub>, the heteroatom class (N<sub>n</sub>O<sub>o</sub>S<sub>s</sub>), type (double bond equivalents, DBE, defined as the number of rings plus double bonds to carbon),<sup>105</sup> and carbon number (*c*) were tabulated for generation of heteroatom class relative abundance distributions and isoabundance-contoured DBE vs carbon number images constructed for each heteroatom class. The molecular weight distribution for each sample was first verified by LTQ analysis to ensure the validity of the molecular weight distribution based on FT-ICR MS.

(88) Cunico, R. L.; Sheu, E. Y.; Mullins, O. C. *Pet. Sci. Technol.* **2004**, *22* (7&8), 787–798.

(89) Groenzin, H.; Mullins, O. C. *J. Phys. Chem. A* **1999**, *103* (50), 11237–11245.

(90) Groenzin, H.; Mullins, O. C. *Energy Fuels* **2000**, *14* (3), 677–684.

(91) Groenzin, H.; Mullins, O. C. Asphaltene molecular size and weight by time-resolved fluorescence depolarization. In *Asphaltenes, Heavy Oils and Petroleomics*; Mullins, O. C., Sheu, E. Y., Hammami, A., Marshall, A. G., Eds.; Springer: New York, 2006; pp 17–62.

(92) Guerra, R.; Andrews, A. B.; Mullins, O. C. *Fuel* **2007**, *86*, 2016–2020.

(93) Merdignac, I.; Espinat, D. *Oil Gas Sci. Technol.* **2007**, *62* (1), 7–32.

(94) Trejo, F.; Ancheyta, J.; Morgan, T. J.; Herod, A. A.; Kandiyoti, R. *Energy Fuels* **2007**, *21* (4), 2121–2128.

(95) Herod, A. A.; Bartle, K. D.; Kandiyoti, R. *Energy Fuels* **2007**, *21*, 2176–2203.

(96) Morgan, T. J.; Morden, W. E.; Al-murareb, E.; Herod, A. A.; Kandiyoti, R. *Energy Fuels* **2006**, *20*, 734–737.

(97) Johnson, B. R.; Bartle, K. D.; Herod, A. A.; Kandiyoti, R. *Prepr. Pap. – Am. Chem. Soc., Div. Fuel Chem.* **1995**, *40* (3), 457–460.

(98) Herod, A. A.; Zhang, S.-F.; Johnson, B. R.; Bartle, K. D.; Kandiyoti, R. *Energy Fuels* **1996**, *10*, 743–750.

(99) Senko, M. W.; Hendrickson, C. L.; Paša-Tolić, L.; Marto, J. A.; White, F. M.; Guan, S.; Marshall, A. G. *Rapid Commun. Mass Spectrom.* **1996**, *10*, 1824–1828.

(100) Schaub, T. M.; Hendrickson, C. L.; Horning, S.; Quinn, J. P.; Senko, M. W.; Marshall, A. G. *Anal. Chem.* **2008**, *80* (11), 3985–3990.

(101) Wilcox, B. E.; Hendrickson, C. L.; Marshall, A. G. *J. Am. Soc. Mass Spectrom.* **2002**, *13*, 1304–1312.

(102) Ledford, E. B., Jr.; Rempel, D. L.; Gross, M. L. *Anal. Chem.* **1984**, *56*, 2744–2748.

(103) Shi, S. D.-H.; Drader, J. J.; Freitas, M. A.; Hendrickson, C. L.; Marshall, A. G. *Int. J. Mass Spectrom.* **2000**, *195/196*, 591–598.

(104) Kendrick, E. *Anal. Chem.* **1963**, *35* (13), 2146–2154.

(105) McLafferty, F. W.; Turecek, F. *Interpretation of Mass Spectra*, 4th Ed.; University Science Books: Mill Valley, CA, 1993; p 371.

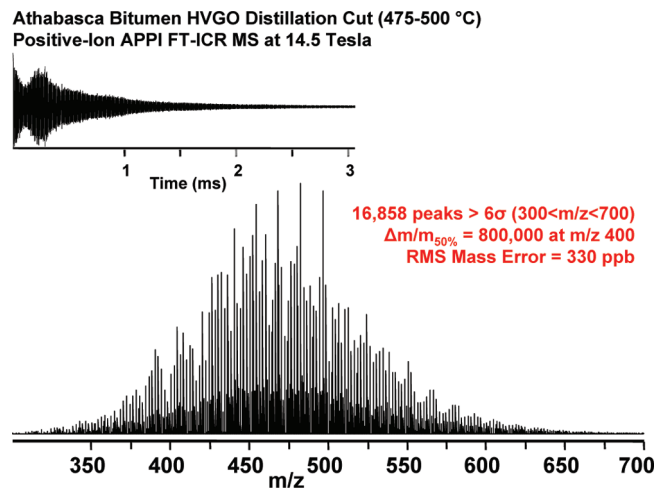


**Figure 2.** Broadband positive-ion atmospheric pressure photoionization (APPI) 14.5 T Fourier transform ion cyclotron resolution mass spectrometry (FT-ICR MS) mass spectrum of an Athabasca bitumen heavy vacuum gas oil (HVGO) distillation cut (475–500 °C). In this figure, 16 858 mass spectral peaks are resolved at 6 times the signal-to-noise ratio baseline root-mean-square (rms) noise at an average resolving power ( $m/\Delta m_{50\%}$ ) of 600 000.

## Results and Discussion

Positive-ion APPI increases mass spectral complexity by the potential formation of two types of ions from a single neutral analyte: radical molecular cations ( $M^{+\bullet}$ ), resulting from the removal of an electron, and  $[M + H]^+$  species due to protonation. For accurate elemental formula assignment, two key isobaric overlaps must be resolved. Species differing in elemental composition by  $C_3$  vs  $SH_4$  both have a nominal mass of 36 Da (but differ by 3.4 mDa in exact mass), are generated by both ESI and APPI, and define the minimum required mass resolving power.<sup>72</sup> However, for APPI of heavy, high-sulfur crude oil, an additional 1.1 mDa doublet arises from  $^{12}C_4$  versus  $SH_3^{13}C$  (both with nominal mass of 48 Da) that must be resolved for correct elemental assignment.<sup>60</sup>

Figure 2 shows a broadband positive-ion APPI FT-ICR mass spectrum for the 475–500 °C distillation cut for an Athabasca bitumen HVGO, containing more than 16 000 peaks (each with a magnitude higher than at least  $6\sigma$  of baseline noise) between 300 and 700 Da, at a mass resolving power ( $m/\Delta m_{50\%}$ , in which  $\Delta m_{50\%}$  denotes the full mass spectral peak width at half-maximum peak height) of 800 000 at  $m/z = 400$ . High mass accuracy alone can provide elemental assignments of peaks below  $\sim 400$  Da. However, Kendrick mass sorting highlights alkylation and hydrogenation patterns that are found in crude oil and allows for unambiguous (mass error of  $< 100$ –300 ppb) assignment of elemental compositions for ions of much higher mass.<sup>72,104,106</sup> Heteroatom class analysis, combined with color-coded isoabundance contour plots of DBE vs carbon number, creates a visual image that is especially helpful for sorting the thousands of elemental compositions into chemically and structurally informative patterns.<sup>106</sup>

**The Boduszynski Hypothesis.** Boduszynski et al. proposed rules to account for the dependence of the boiling point on

the molecular weight and elemental composition for organic components of heavy crude oil.<sup>2,3</sup> A fundamental principle is “diverse compounds with similar molecular weights cover a broad boiling range; and conversely, a narrow boiling point cut can contain a wide molar mass range”.<sup>2,3</sup> Figure 1 shows plots of molecular mass versus atmospheric equivalent boiling point (AEBP), yielding positive-sloped, wedge-shaped envelopes for each compound type. For a given boiling point, the highest molecular weight components are paraffins, followed by naphthenes, aromatic hydrocarbons, heteroatom-containing compounds, polar heteroatom-containing compounds, and finally polar, unsubstituted aromatic heteroatom-containing compounds.<sup>2,3</sup> Vertical progression from one compound class to the next reveals a difference of 2–3 C atoms per molecule at a given boiling point. For example, an unsubstituted polycyclic aromatic hydrocarbon (PAH) from a low-boiling HVGO cut (427 °C) contains  $\sim 17$ –18 C atoms per molecule. Monoheteroatomic compounds with the same boiling point, such as  $S_1$  or  $N_1$  classes, contain  $\sim 2$ –3 fewer C atoms per molecule than their PAH analogs. Compounds with two heteroatoms at that same boiling point contain  $\sim 5$ –6 fewer C atoms than their PAH analogs. A polar, polyfunctional heteroatom-containing compound molecule would contain 6–7 fewer C atoms than its PAH analog of the same boiling point. Boduszynski proposed that the most polar compounds with the highest heteroatom content at a specific mass would have the highest boiling point; conversely, hydrocarbons (devoid of heteroatoms) would have the lowest boiling point for a given mass.<sup>2,3</sup> Table 1 shows boiling point data for several types of core structure known to exist in crude oil.

**Compositional Differences among HVGO Distillate Cuts: Tests of the Boduszynski Hypothesis.** We compared Boduszynski’s predictions with experimental carbon number distributions obtained by ESI and APPI FT-ICR MS for a series of distillation cuts varying by  $\sim 25$  °C increments. Figure 3 shows isoabundance-contoured plots of DBE vs carbon number for members of the hydrocarbon class for all eight distillate fractions from the initial boiling point (IBP) to 538 °C. An increase in abundance-weighted average carbon number accompanies an increase in boiling point, from  $\sim 20$  carbons for the lightest fraction (IBP–343 °C) to  $\sim 40$  C atoms for the highest-boiling fraction (500–538 °C). Each 25 °C increase in boiling point results in the addition of  $\sim 1$ –4 C atoms to the average carbon number. The large 6-carbon-number increase from IBP–343 °C to 343–375 °C most likely is due to the wide boiling point range associated with the vaguely defined “initial boiling point”. A similar jump (from  $\sim C_{30}$  to  $\sim C_{38}$ ) occurs in the final distillation cut, because the final cut has an undefined upper limit in boiling point.

Progression from the first to the last well-defined boiling cuts (343–375 °C to 475–500 °C) results in a gradual increase from 26 carbons to 35 carbons in increments of 1 or 2 carbons. Careful scrutiny of the fractions above the 343–375 °C cut reveals a slight widening of the carbon number distribution toward lower carbon number for the most-abundant, higher-DBE species. The shift tilts the otherwise-vertical distributions slightly to the left. That behavior highlights a fundamental principle of the Boduszynski model: as the aromaticity (and, thus, DBE) increases, the number of carbons for the more aromatic species must decrease to remain in the same distillation cut. However, the tilt diminishes in the highest boiling fractions, presumably because of the increased structural

(106) Hughey, C. A.; Hendrickson, C. L.; Rodgers, R. P.; Marshall, A. G.; Qian, K. *Anal. Chem.* **2001**, *73* (19), 4676–4681.

degeneracy in and between aromatic and cycloalkane species at higher DBE, as well as variation in ionization efficiency and dynamic range limitations at increased levels of compositional complexity (increased boiling point). The number-average DBE (aromaticity) also increases, from compounds with

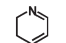
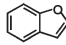
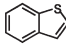
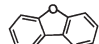
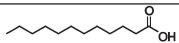
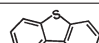
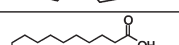
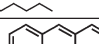
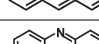
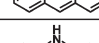
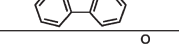
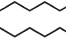
DBE = 7 (the IBP–343 °C fraction) to DBE = 10 (the 500–538 °C fraction). An increase in aromaticity accompanied by an increase in boiling point matches the increase in carbon number predicted by Boduszynski et al.<sup>2,3</sup> Based on that model, the hydrocarbon class (compounds with no heteroatoms) should exhibit the highest molecular weight for a given boiling point.

Figure 4 shows DBE vs carbon number images for the S<sub>1</sub> class spanning the HVGGO distillation series. As for the hydrocarbon class, the carbon number increases from ~18 (for the IBP–343 °C cut) to ~39 (for the 500–538 °C cut). Again, the most pronounced difference in carbon number occurs between the lightest (heaviest) cut and the next-nearest cut. The average molecular weight again increases steadily with increasing boiling point, and the tilt to the left at high DBE indicates that higher DBE species of the same boiling point must have slightly lower carbon numbers.

The compositional dependence on boiling point is further elucidated by the DBE vs carbon number images for the S<sub>2</sub> class (see Figure 5). The average carbon number jumps from C<sub>17</sub> to C<sub>22</sub> from the lowest to next-highest boiling point cut, but steadily increases thereafter to a maximum of C<sub>38</sub> for the highest-boiling cut. Similar plots for all 10+ classes in the bitumen HVGGO distillation series reveal identical trends. All classes exhibit an abnormally high increase in carbon number from the IBP fraction to the 343–375 °C cut with steadily increasing carbon numbers through cuts 2–7 and another increase from the 475–500 °C cut to the 500–538 °C cut.

Comparison of the average carbon number in each distillate cut *between* classes (hydrocarbon, S<sub>1</sub>, and S<sub>2</sub>) provides clinching support for the Boduszynski model. Specifically, each heteroatom addition (from hydrocarbon to S<sub>1</sub> and then to S<sub>2</sub>) results in a decrease in ~2–3 C atoms within a given boiling point range from the hydrocarbon (Figure 3) to S<sub>1</sub> (Figure 4) and finally, the S<sub>2</sub> class (Figure 5). For example,

**Table 1. Structures and Boiling Point for Representative Crude Oil Compounds**

Name	Formula	Structure	T <sub>boil</sub> (°C)*
Pyridine	C <sub>5</sub> H <sub>5</sub> N		115.3
Benzofuran	C <sub>8</sub> H <sub>6</sub> O		174.1
Benzothiophene	C <sub>8</sub> H <sub>6</sub> S		221.1
Dibenzofuran	C <sub>12</sub> H <sub>8</sub> O		285.1
Lauric acid	C <sub>12</sub> H <sub>24</sub> O <sub>2</sub>		297.9
Dibenzothiophene	C <sub>12</sub> H <sub>8</sub> S		332.5
Palmitic acid	C <sub>16</sub> H <sub>32</sub> O <sub>2</sub>		339.3
Anthracene	C <sub>14</sub> H <sub>10</sub>		340.1
Acridine	C <sub>13</sub> H <sub>9</sub> N		345.5
Carbazole	C <sub>12</sub> H <sub>9</sub> N		355.1
Stearic Acid	C <sub>18</sub> H <sub>36</sub> O <sub>2</sub>		361.1
Coronene	C <sub>24</sub> H <sub>12</sub>		525.1

\* Boiling point data from www.nist.org.

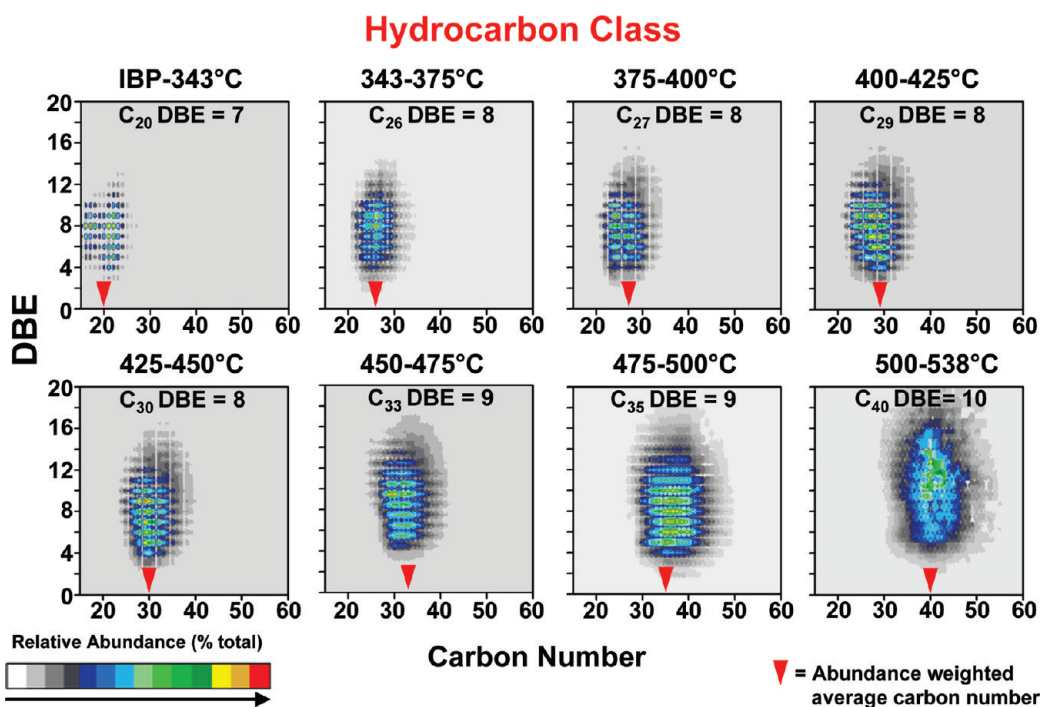


**Figure 3.** Color-coded isoabundance contoured plots of DBE vs carbon number for the hydrocarbon class for Athabasca bitumen HVGGO distillate cuts. The carbon number abundance distribution maximum (red arrow) shifts from ~C<sub>20</sub> at IBP–343 °C to ~C<sub>40</sub> at 500–538 °C. DBE values show a gradual increase in aromaticity from DBE ≈ 7 to DBE ≈ 10 with increasing boiling point.



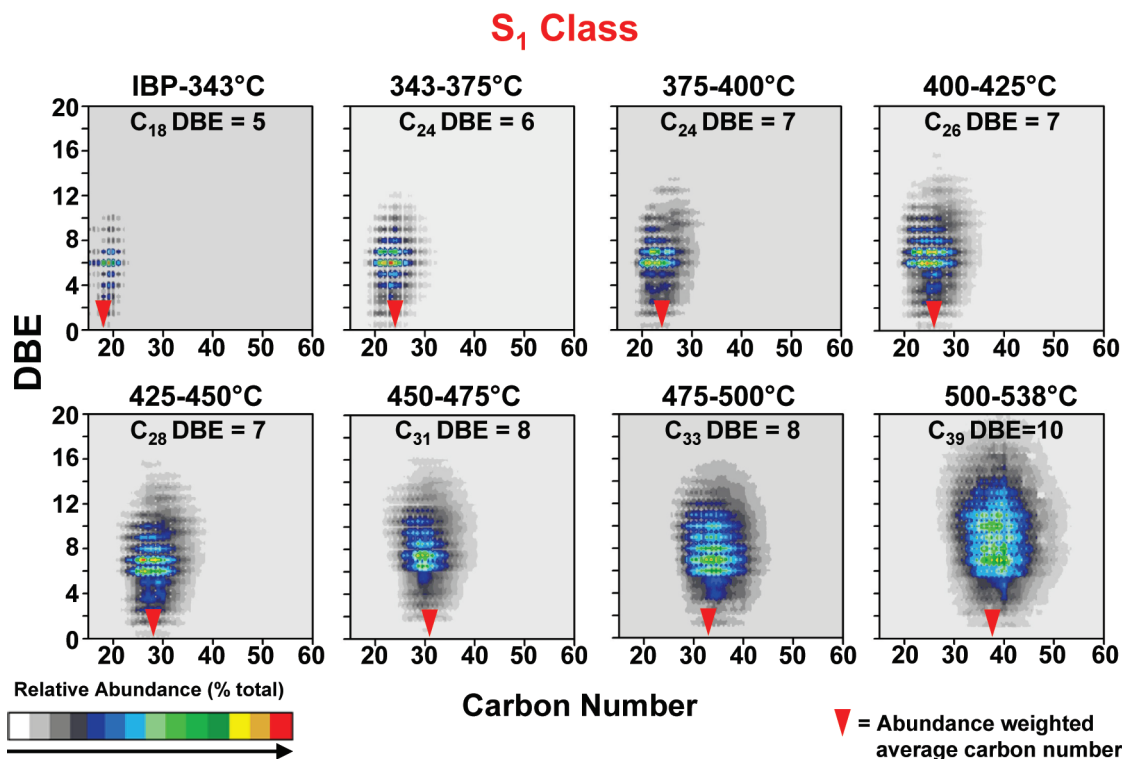


**Figure 4.** DBE versus carbon number images for the S<sub>1</sub> class for Athabasca bitumen HVGO distillate cuts. The carbon number abundance distribution maximum shifts from ~C<sub>18</sub> at IBP–343 °C to ~C<sub>39</sub> at 500–538 °C but for ~2 fewer carbons than for pure hydrocarbon analogues (recall Figure 3). DBE values increase from DBE ≈ 5 to DBE ≈ 10 with increasing boiling point, as for the hydrocarbon class.

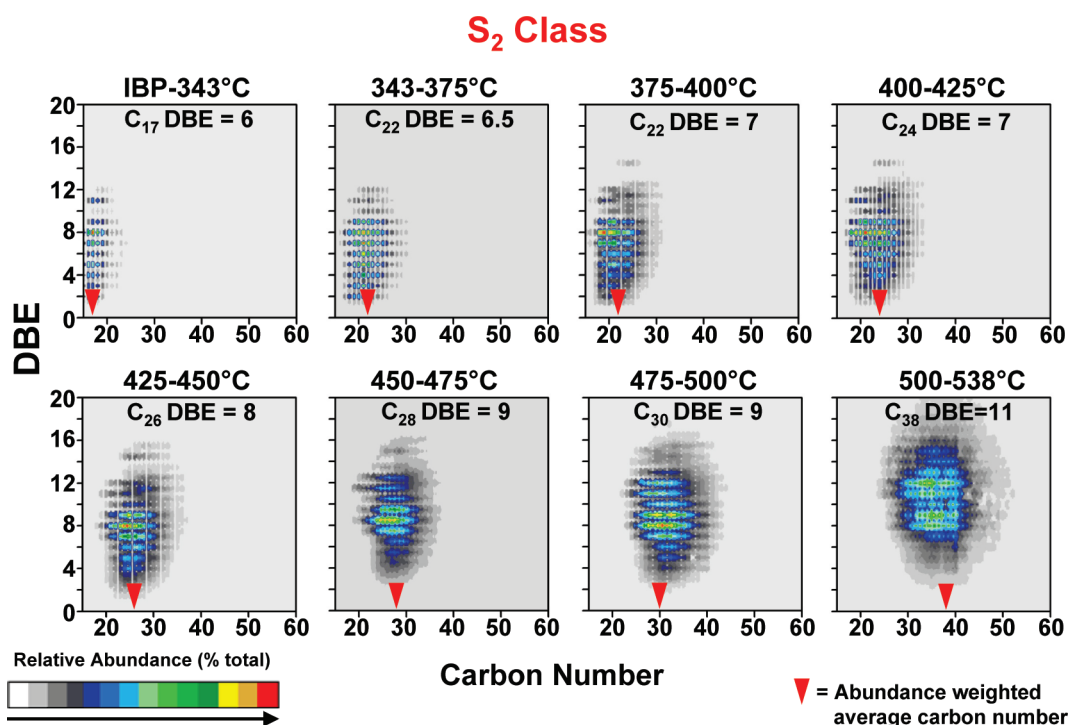


**Figure 5.** DBE versus carbon number images for the S<sub>2</sub> class for Athabasca bitumen HVGO distillate cuts. The carbon number abundance distribution maximum shifts from ~C<sub>18</sub> at IBP–343 °C to ~C<sub>39</sub> at 500–538 °C but for ~2 fewer carbons than the S<sub>1</sub> class (recall Figure 4) and ~4 fewer carbons than the hydrocarbons class (recall Figure 3). DBE values increase similarly, from DBE ≈ 6 to DBE ≈ 11, with increasing boiling point.

the hydrocarbon class for the 450–475 °C cut exhibits an average carbon number of 33. For the same boiling cut, the addition of a S atom shifts the average carbon number to 31.

Similar trends are readily apparent for all distillate fractions, directly validating the Boduszynski model. The distillate results for the 343–450 °C distillate ranges (4 cuts) are

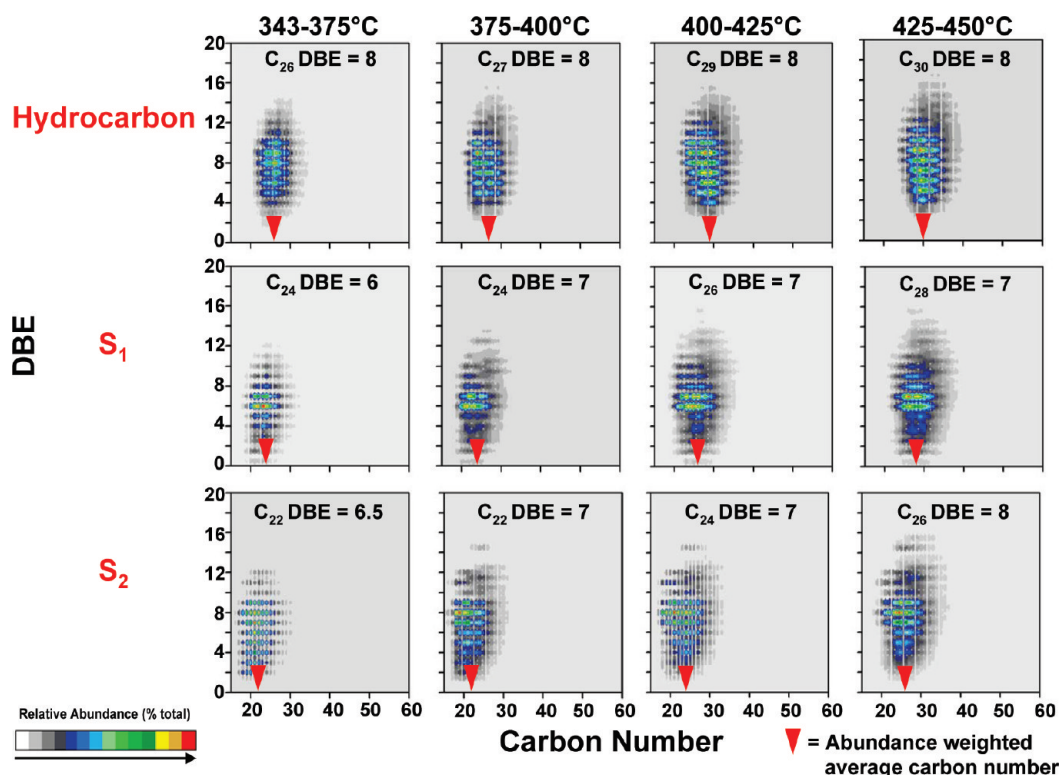


**Figure 6.** Composite DBE versus carbon number images for the hydrocarbon,  $S_1$ , and  $S_2$  classes for four of the eight HVGO distillate fractions shown in Figures 3, 4, and 5. Within each boiling range, each increase in one S atom shifts to lower carbon number which corresponds to results in  $\sim 2\text{--}3$  fewer carbons per structure.

collected for the hydrocarbon,  $S_1$ , and  $S_2$  classes in Figure 6. Progression from the hydrocarbon class to the  $S_1$  and  $S_2$  classes yields the predicted decrease of 2–3 carbons for all four distillate cuts. For a given distillate cut, progression from a hydrocarbon to monoheteroatom-containing species decreases the number of carbons by 2–3. Going from a monoheteroatom-containing ( $S_1$ ) to a diheteroatom-containing ( $S_2$ ) class, the carbon number decreases by another 2–3. Importantly, trends in carbon number and aromaticity, accompanied by increased heteroatom content, as a function of boiling point, are *gradual* and *continuous* within and between all classes and match those proposed by Boduszynski.

Summarized another way, Figure 7 illustrates the relationship between heteroatom class (hydrocarbon,  $S_1$ ,  $S_2$ , and  $S_1O_1$ ) and boiling point for a *fixed* carbon number ( $\sim 25$ ). It is clear that, for a given molecular weight (carbon number) each additional S atom corresponds to an increase of  $\sim 25^\circ\text{C}$  in boiling point. Finally, although the  $SO$  and  $S_2$  classes both contain two heteroatoms per molecule, the increased polarity of the  $S_1O_1$  class displays a higher boiling point than the (likely) dithiophenic  $S_2$  class. In addition, a decrease in aromaticity is noted for the  $S_1O_1$  class. That behavior is predicted by Boduszynski, because polar atoms such as oxygen are capable of hydrogen bonding and can participate in other polar interactions that result in a higher boiling point.<sup>107</sup>

Differences in DBE and carbon number among nonpolar hydrocarbon and  $S_1$  classes and polar, acidic  $O_2$  species are shown in Figure 8. (Because carboxylic compounds represent a small fraction of the heteroatom classes present in

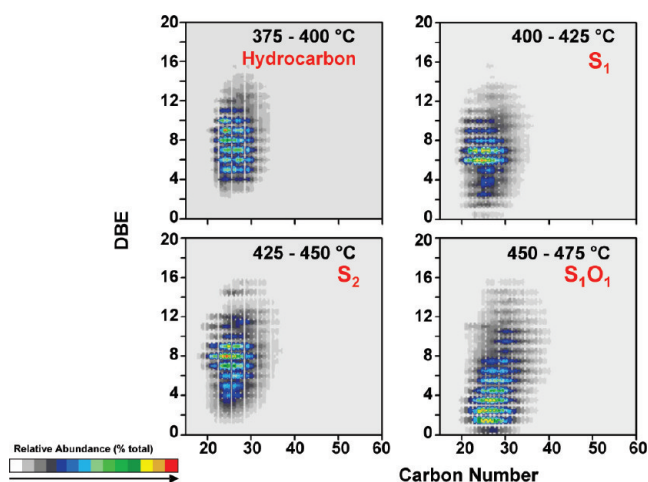


**Figure 7.** DBE versus carbon number images for four distillation cuts. Here, for a given carbon number ( $\sim 24\text{--}25$ ), each additional heteroatom is observed to increase the boiling point by  $\sim 25^\circ\text{C}$ .

crude oil, they are lower in relative abundance, as analyzed by positive-ion APPI. Therefore, to selectively ionize only acidic species for direct comparison with nonpolar hydrocarbons and thiophenes, data for the  $O_2$  class were acquired by negative-ion ESI 9.4 T FT-ICR MS. For the 425–450  $^\circ\text{C}$  boiling cut, the average carbon number decreases by two carbons (from  $\sim C_{30}$  for hydrocarbons to  $\sim C_{28}$  for the  $S_1$  class). Proceeding from a monoheteroatom-containing species ( $S_1$ ) to a highly polar diheteroatom-containing species ( $O_2$ ) results in a slightly lower carbon number ( $\sim C_{27}$ ) but a large drop in the aromaticity from DBE = 7 to DBE = 4,

(107) Boduszynski, M. M.; Altgelt, K. H. *Composition and Analysis of Heavy Petroleum Fractions*; CRC Press: New York, 1994.



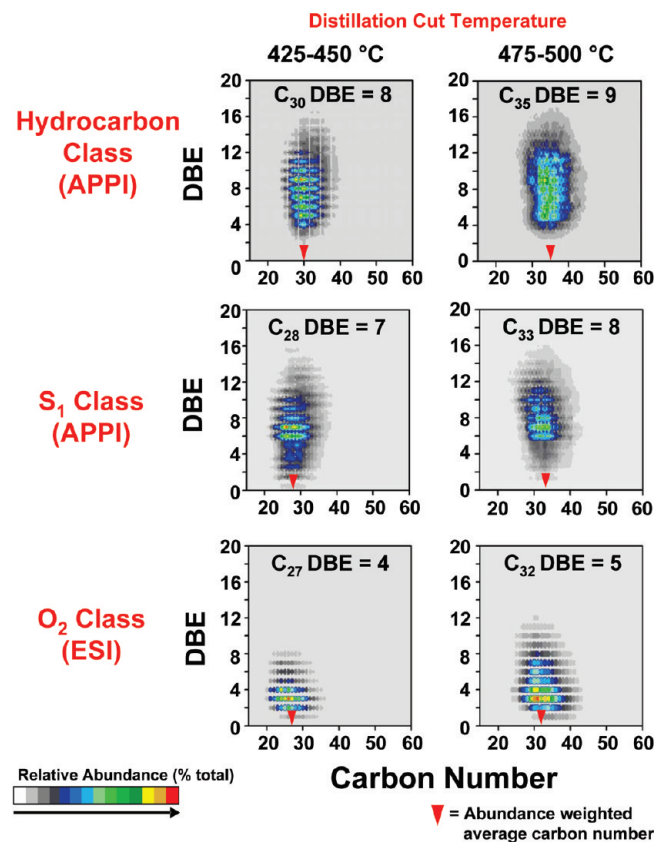


**Figure 8.** DBE vs carbon number images for the hydrocarbon (APPI), S<sub>1</sub> (APPI), and acidic O<sub>2</sub> (ESI) classes from the 425–450 °C and 475–500 °C HVGO distillation cuts of whole Athabasca bitumen. Proceeding from hydrocarbon to S<sub>1</sub> for either cut, the carbon number decreases by 2. Polar O<sub>2</sub> classes, most likely from carboxylic functionalities, contain three fewer carbons than hydrocarbons and one fewer carbon than monoheteroatomic S<sub>1</sub> classes.

because polar compounds exhibit stronger intermolecular forces that result in higher boiling points at a given molar mass. Thus, acidic O<sub>2</sub> species display slightly lower molecular weights and strikingly lower aromaticity than their non-polar counterparts for each boiling cut. Similar trends were noted for both acidic and basic species across distillation range.

**The HVGO Compositional Continuum.** To further illustrate the continuity of HVGO compositional variation with boiling point, we combined data for the hydrocarbon class for each boiling point fraction into a single DBE vs carbon number image (see Figure 9). Relative abundances for each distillate fraction were scaled to 100 as the highest-magnitude peak for direct comparison between boiling points. As the boiling point increases, the carbon number shifts continuously from ~C<sub>15</sub> (IBP–343 °C) to ~C<sub>55</sub> (500–538 °C). The high abundance of relatively low-molecular-weight species (>C<sub>20</sub>) has been discussed previously and is attributed to the lack of a well-defined starting temperature for the lowest-boiling fraction. Carbon number increases gradually from ~C<sub>22</sub> for boiling cuts defined in the HVGO temperature range. Aromaticity also gradually increases from DBE ≈ 2 to DBE ≈ 20 (an average of ~3–4 aromatic rings). All other heteroatom classes identified by positive-ion APPI and positive/negative-ion ESI resulted in similar plots. These results irrefutably demonstrate that crude oil is continuous

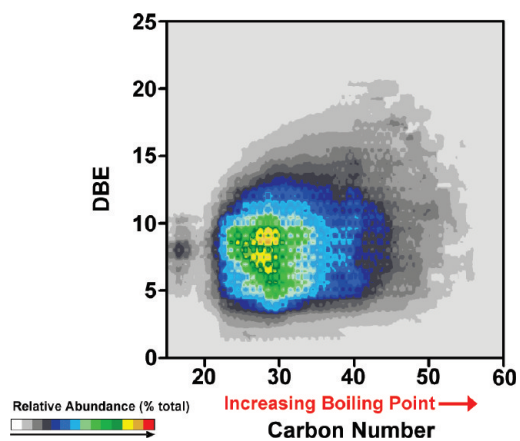


**Figure 9.** Combined DBE versus carbon number images for all distillation cuts combined for the hydrocarbons class from Athabasca bitumen HVGO. Carbon number and DBE values increase monotonically with increasing boiling point across the entire series. The Boduszynski model is irrefutably supported by this figure: the crude oil composition is continuous, with regard to carbon number, DBE, and boiling point.

in composition, structure, and boiling point across the HVGO temperature range.

**Cycloalkane Ring Addition.** Characterizing the structure of high-boiling, highly polar compounds such as asphaltenes and resins requires a thorough understanding of the structural progression of lower-boiling crude oil compounds. Bitumen is also referred to as “extra-heavy oil” and contains ~15%–17% asphaltenes (by weight) with a viscosity of > 100 000 cP and API gravity of 7°–15°.<sup>108,109</sup> To characterize species found in the heaviest crude oil ends, we first examine the combined bitumen HVGO fractions and note the structural progression of aromatic ring systems by APPI FT-ICR MS.

Figure 10 shows DBE vs carbon number images for the hydrocarbon S<sub>1</sub> class for HVGO derived from Athabasca bitumen. Thiophene corresponds to a DBE value of 3. The addition of one or two phenyl rings yields benzothiophene (DBE = 6) and dibenzothiophene (DBE = 9) core structures. However, they do not exhibit high relative abundance for DBE “magic number” values corresponding to those aromatic cores, and there are many species with intermediate DBE values. The intermediate DBE values cannot be due to alkene linkages, because alkenes are not found in crude oil.<sup>110</sup> Also, APPI can result in proton transfer, which changes the DBE by 0.5 but does not affect the present argument.<sup>111</sup> Thus, cycloalkane ring addition must account for the species found with DBE values of 4–5 and 7–8, and HVGO suggests that the progression in DBE occurs through the addition of cycloalkane rings. The effect is most easily evident at low DBE values, where structural degeneracy in aromatics is minimized. At higher DBE values, the possibility of multiple structural isomers clouds the assignment of integer DBE value increments. Whether or not the cycloalkane-substituted aromatic structural motif extends

(108) Berkowitz, N.; Speight, J. G. *Fuel* **1975**, *54*, 138–149.

(109) Chow, D. L.; Nasr, T. N.; Chow, R. S.; Sawatzky, R. P. *J. Can. Pet. Technol.* **2008**, *47* (5), 12–17.

(110) Lawrence, E. O.; Livingston, M. S. *Phys. Rev.* **1931**, *38* (4), 834–834.

(111) Rodgers, R. P.; McKenna, A. M.; Purcell, J. M.; Smith, D. F.; Marshall, A. G. *Prepr. Pap.—Am. Chem. Soc., Div. Pet. Chem.* **2008**, *53* (2), 151–153.

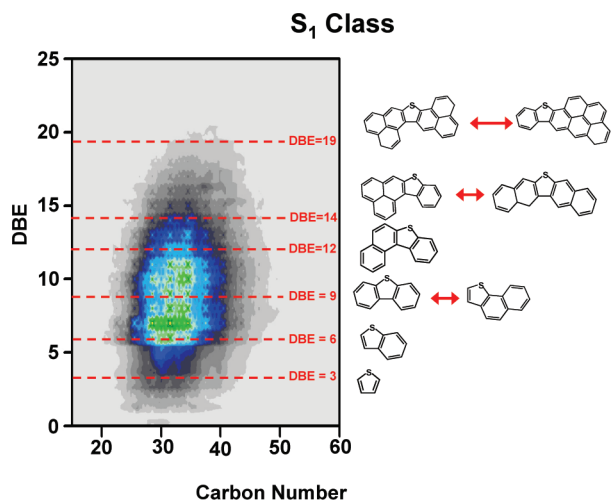


**Figure 10.** DBE versus carbon number images for the S<sub>1</sub> class of the Athabasca bitumen HVGO feedstock for all distillation cuts combined. The number of aromatic rings corresponding to various DBE values are shown for representative structures. Because the abundance distribution is monomodal (i.e., no “magic numbers”), including significantly abundant species with DBE values intermediate between those of fused aromatic rings, cycloalkyl-ring addition must be invoked to account for the intermediate DBE values.

into the heavy ends and asphaltenes has yet to be demonstrated by high-resolution MS. Nevertheless, the Boduszynski model predicts that the seeds of structural diversity in the lower-boiling fraction augur that the continuity model demands their presence in the heavier ends. If large condensed aromatic ring systems indeed occur in heavy crude oil and are bridged by cycloalkane or heteroatom-containing 5-membered rings, it should be possible to crack across those linkages to yield the distillable hydrocarbons produced in heavy end and asphaltene conversion. We are currently exploring that possibility.

Detailed compositional characterization of a heavy vacuum gas oil (HVGO) distillation series exposes the relationship between molecular weight, aromaticity, and boiling point. More than 150 000 mass spectral peaks provided elemental compositions with mass errors of <400 ppb and allowed the calculation of double-bond equivalent (DBE) values, and Kendrick sorting identified homologous series within each distillation cut. Within each heteroatom class, an increase in carbon number increases the boiling temperature. Among classes for a given boiling point, the compositional changes (carbon number and DBE) conform closely to the Boduszynski model, even for polar species. The DBE versus carbon number image “tilt” suggests that the highest DBE species must have fewer carbons to reside in the same distillate cut with heavier, less-aromatic species. However, that trend becomes less pronounced as the complexity (boiling point) of the cut increases, most likely because of a pronounced increase in the number of possible structures that contain combinations of aromatic and cycloalkane moieties. The lack of “magic” DBE values corresponding to polyaromatic cores (e.g., thiophene, DBE = 3; benzothiophene, DBE = 6; and dibenzothiophene, DBE = 9), even at low DBE, suggests the importance of cycloalkane structures in the overall contribution to DBE.

In summary, we have provided detailed, comprehensive analysis of compositional trends within the HVGO boiling range to provide the first definitive evidence for the validity and accuracy of the Boduszynski model. In the next paper in this series, we shall extend our analysis through the distillation upper limit and into nondistillable residues.

**Acknowledgment.** This work was supported by NSF Division of Materials Research (through DMR-0654118) and the State of Florida. The authors thank Dr. Parviz Rahimi at the National Centre for Upgrading Technology for providing and fractionating the bitumen samples. The authors also thank Shell Global Solutions, Houston, TX, for financial support.